Available online at www.sciencedirect.com
SCIENCE DIRECT
Polymer 46 (2005) 2558–2566
polymer
www.elsevier.com/locate/polymer

Synthesis and characterization of (star polystyrene)-*block*-(polyisoprene)-*block*-(star polystyrene) copolymers

Mei-Kuan Lai, Jyr-Ynna Wang, Raymond Chien-Chao Tsiang*

Department of Chemical Engineering, National Chung Cheng University, Ming-Hsiung, Chiayi 621, Taiwan, Republic of China

Received 15 September 2004; received in revised form 23 January 2005; accepted 25 January 2005

Abstract

A (star polystyrene)-*block*-(linear polyisoprene)-*block*-(star polystyrene) copolymer, $(S)_nI(S)_n$, was prepared. The star polystyrene was produced via anionic polymerization of polystyrene macromonomers each containing an unsaturated double bond (vinyl) at the chain end. This vinyl-terminated polystyrene macromonomer (SSTM) was obtained beforehand via the synthesis of a living polystyrene using alkyllithium and the termination with *p*-chloromethylstyrene (PCMS). The living site in the core of the star polystyrene enabled the construction of the succeeding polyisoprene block resulting in the living (star polystyrene)-*block*-(linear polyisoprene) copolymer, $(S)_nI$. This living diblock copolymer was then coupled with 1,2-dibromoethane (DBE) to form the well-defined $(S)_nI(S)_n$. Compared to a linear polystyrene-*block*-polyisoprene-*block*-polystyrene, SIS, with the same molecular weight, $(S)_nI(S)_n$ had a higher T_g and exhibited a lamellae-forming phase separation in conjunction with many dislocation defects. The thermal stability appeared independent of the molecular structure, and the radius of gyration and viscosity of $(S)_nI(S)_n$ were much smaller than SIS.

Keywords: Pom–pom polymers; Anionic polymerization; Polyisoprene

1. Introduction

The syntheses of architectural block copolymers have gained considerable interest due to the great technological importance of these materials in applications such as thermoplastic elastomers, compatibilizers for polymer blends, and modifiers for surface and interfacial properties, etc [1]. Copolymers with segments of complex branch architecture, often result in materials with unique properties.

Various architectural block copolymers such as the H-shaped polymers [2–5] and the super-H-shaped polymers (i.e. the bridged star polymers) [6–8] have been synthesized and their dilute solution properties and melt properties have been studied and compared to their linear analogues [2,9]. These A_nBA_n block copolymers were synthesized by a variety of multiple-step methods with some multifunctional coupling agent, and the number of arms in the end block, n, was generally small [10–14]. Recently, pom–pom polystyrenes with identical star blocks at each end of a linear block were sequentially synthesized by Knauss and Huang via the convergent living anionic polymerization [15,16]. This sequential synthesis involved first the formation of a living anionic star polystyrene with a hyperbranched core via continuous addition of the coupling agent, 4-(chlorodimethylsilyl)styrene, to living polystyrene chains. Subsequent addition of styrene monomer to the living star polystyrene anions produced the $(S)_nS$ diblock polystyrene anions that were then coupled with dichlorodimethylsilane to make the $(S)_nS(S)_n$ triblock architecture. This convergent living anionic polymerization method enabled the syntheses of pom–pom polymers with a n as high as 11, depending upon the molecular weight of the arm of the star blocks.

In this article, (star polystyrene)-*block*-(linear polyisoprene)-*block*-(star polystyrene) copolymers, $(S)_nI(S)_n$, was synthesized via an alternate sequential method. The initial synthesis of living polystyrene was based on typical anionic

* Corresponding author. Tel.: +886 5 2428122; fax: +886 5 2721206.
E-mail address: chmcct@ccu.edu.tw (R.C.-C. Tsiang).

0032-3861/$ - see front matter © 2005 Elsevier Ltd. All rights reserved.
doi:10.1016/j.polymer.2005.01.042

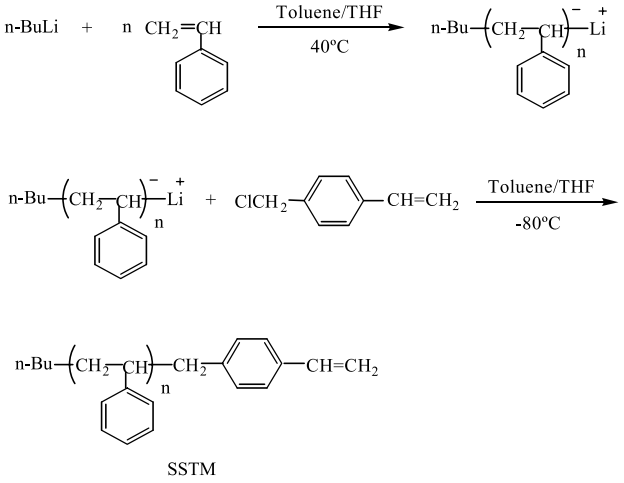

Scheme 1. SSTM synthesis.

polymerization procedures. The vinyl-terminated polystyrene macromonomer (SSTM) was then formed via a termination of the living polystyrene with *p*-CMS [17,18]. This vinyl-terminated polystyrene was then used to construct a well-defined star polystyrene, with a living site capable of the succeeding polymerization of isoprene leading to the formation of $(S)_nI$ diblock anions [19]. Finally $(S)_nI(S)_n$ was synthesized via the coupling of the $(S)_nI$ diblock anions with 1,2- dibromoethane (DBE) [20]. The linear polyisoprene middle block conferred unusual and distinct properties on $(S)_nI(S)_n$. The structure of $(S)_nI(S)_n$ was characterized by ^1H NMR and gel permeation chromatograph, and the thermal and rheological properties were compared to a linear analogue using the multiple-angle laser light scattering, the thermogravimetric analyzer, the differential scanning calorimeter, the transmission electron microscope and the rheometer.

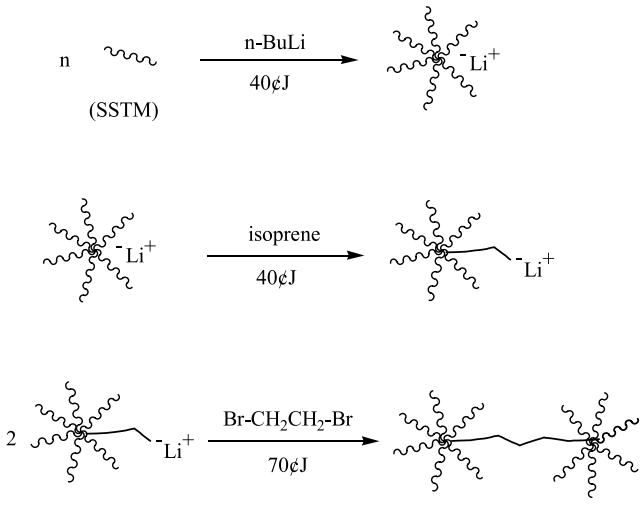

Scheme 2. Pom–pom copolymers $(S)_nI(S)_n$ synthesis.

2. Experimental

2.1. Materials

Styrene used in this work was obtained from Taiwan Synthetic Rubber Corp. and was pretreated with activated alumina (Alcoa Co.) before it was used. Isoprene was purchased from Merck (KGaA, Darmstadt, Germany), purified by distillation, and soaked in activated alumina before it was used. *n*-BuLi was obtained from Taiwan Synthetic Rubber Corp. as a 15 wt% solution in hexane. HPLC grade tetrahydrofuran (THF) was purchased from JTB, dried over sodium metal, and distilled from sodium benzophenone ketyl under nitrogen. *p*-Chloromethyl styrene (*p*-CMS) was purchased from Fluka Chemie GmbH and was pretreated with activated alumina before it was used. 1,2-dibromoethane (DBE) was purchased from Merck (KGaA, Darmstadt, Germany) and was used as the coupling agent. Solvents and other reagents were purified by conventional methods.

2.2. Polymer syntheses

The route of SSTM synthesis is shown in Scheme 1. To a 500 ml pressure vessel under a slight nitrogen overpressure were added 200 ml toluene and THF (20/3 volume ratio, Toluene/THF). Styrene (12–16 ml) was then polymerized at 40 °C for 1 h in this vessel with 5 ml *n*-BuLi as the initiator. The initiation efficiency of *n*-BuLi had been determined as 0.85 from a test run conducted prior to this formal run (via a comparison of the kinetic molecular weight with the targeted molecular weight). The color became reddish orange, and this indicated the presence of living polystyryllithium anions. *p*-CMS, amounting to 1.5 mol of *p*-CMS/mol of living polystyryllithium, was next added to this vessel, and SSTM was formed via a capping reaction at −80 °C for 3 h. The increase in the solvent polarity due to the addition THF increased the capping efficiency [21], and the low synthesis temperature prevented the undesired cycloeliminative reaction of THF [22]. After the completion of the capping reaction, the vessel content was poured into a NaOH solution and stirred for 2 h, followed by repeated washes with distilled water. The organic layer was separated from the aqueous layer and poured into a large amount of isopropyl alcohol to precipitate the SSTM. The precipitated SSTM was dried in vacuum at 40 °C and then washed with methanol to remove the residual *p*-CMS in an extraction apparatus for 24 h.

The route of synthesis for pom–pom copolymers $(S)_nI(S)_n$ is shown in Scheme 2. First, the star polystyrenes $(S)_n$ were prepared by the anionic polymerization of the SSTM in 200 ml toluene at 40 °C for 3 h with *n*-BuLi (with an initiation efficiency of 0.85) as the initiator. The number of arms of star $(S)_n$ was made exact via the precise control over the molar ratio of SSTM to *n*-BuLi [23]. Next, isoprene was added to the living $(S)_n$ to continue the anionic

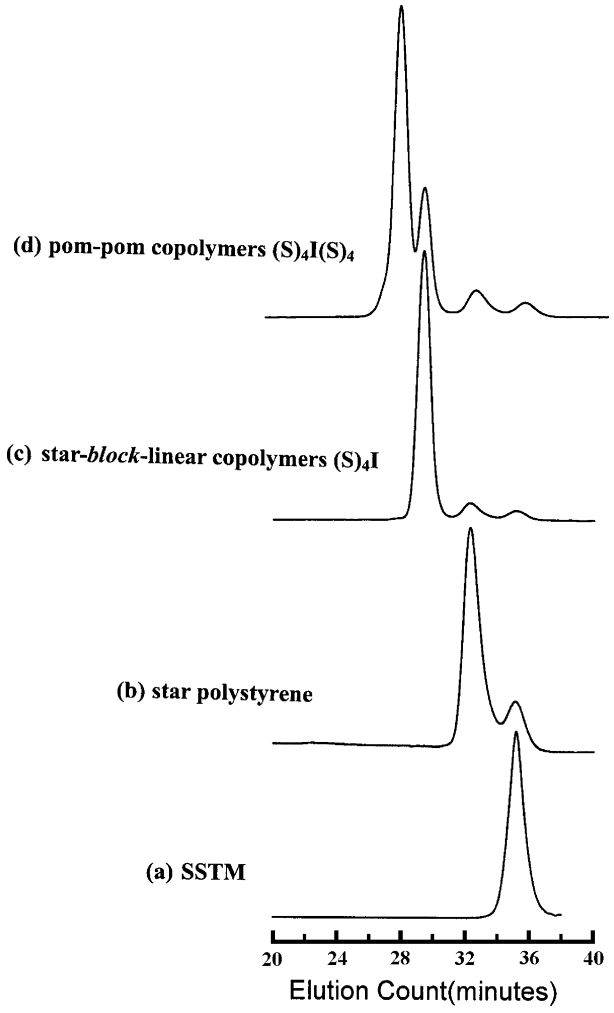

Fig. 1. Variation in the molecular weight distribution during the synthesis of $(S)_4I(S)_4$.

polymerization at 40 °C for 3 h, resulting in the formation of $(S)_nI$. The content ratio of styrene and isoprene in the polymer was fixed at a number of either 3/7 or 4/6. Finally, 1,2-dibromoethane, in an amount of 1.25 molar ratio to *n*-BuLi, was added for coupling. After the completion of the coupling reaction, the vessel content was poured into a large amount of isopropyl alcohol to precipitate the ultimate products. The precipitated $(S)_nI(S)_n$ was then dried in vacuum at 40 °C for 72 h.

2.3. Analysis of the synthesized polymers

The molecular structures of the SSTM and $(S)_nI(S)_n$ were determined with NMR spectroscopy. The ^1H NMR spectra of the polymers were taken with a BRUKER AMX 400 spectrometer. The relative molecular weights and the molecular weight distributions of the synthesized polymers were determined with a Waters gel permeation chromatograph equipped with the Waters 410 differential RI detectors (GPC-RI). The GPC was operated using four Waters Styragel HR Columns (HR0.5, HR3, HR4, HR5E) at a nominal flow rate of 1 ml/min with a sample concentration of 0.1% in THF solvent. Monodisperse polystyrene standards were purchased from Polymer Laboratories (UK) for instrument calibration. The absolute molecular weight of the $(S)_nI(S)_n$ was determined with the GPC-MALLS instrument (mini-DAWN model, Wyatt Technology Corp. equipped with a 20 mW semiconductor laser at a 690 nm wavelength). The molecular weight determination with GPC-MALLS necessitated the measurement of the specific RI increment (d*n*/d*c*). The d*n*/d*c* value of the synthesized polymer, at the same wavelength of light as MALLS, was measured with a Wyatt/Optilab DSP interferometric refractometer. Thermogravimetric analyzer (TGA) analyses were performed with a Dupont TA Instrument Co. (TGA 2050). The TGA analyses of the synthesized polymers were conducted at a heating rate of 10 °C/min from 30 to 500 °C with dry nitrogen as the effluent gas. The thermal analyses were performed with a differential scanning calorimeter (Dupont TA Instrument Co.-2910 Modulated DSC). The samples were heated from −100 to 150 °C at a heating rate of 10 °C/min with dry nitrogen as the effluent gas (60 ml/min). Transmission electron microscopy (TEM) analyses were conducted on a Hitachi H-700H TEM system. The specimen for the measurements was prepared by cutting into slices (50 nm) using ultrathin microtome beforehand. Rheology was measured with a rheometer (Dupont TA Instrument Co.-AR1000) [24].

3. Results and discussion

3.1. Synthesis

The GPC-RI chromatograms of the samples taken at the completion of each step during the synthesis of $(S)_4I(S)_4$ are shown in Fig. 1. Fig. 1(a) is for the linear SSTM chains. In Fig. 1(b), the left peak at the lower elution time corresponded to the star polystyrenes $(S)_4$ arising from the anionic polymerization of the SSTM, and the right peak at the higher elution time corresponded to the unreacted SSTM chains. The molecular weight of the $(S)_4$ was nearly fourfold of the molecular weight of the linear SSTM chains via a precise control of the molar ratio of SSTM to *n*-BuLi [23]. The conversion ratio of SSTM into $(S)_4$ was determined as 82.3% from the GPC chromatogram in Fig. 1(b) based on magnitudes of the areas underneath the two peaks. After an addition of isoprene to continue the polymerization, the left peak shifted toward left indicating the conversion of $(S)_4$ into $(S)_4I$, as shown in Fig. 1(c). The conversion ratio of $(S)_4$ into $(S)_4I$ determined from the GPC chromatogram in Fig. 1(c) was 94.9%. After the coupling reaction with DBE, $(S)_4I(S)_4$ appeared as the left most peak in Fig. 1(d). Moreover, the molecular weight of the $(S)_4I(S)_4$ was twice as large as the molecular weight of $(S)_4I$. The coupling

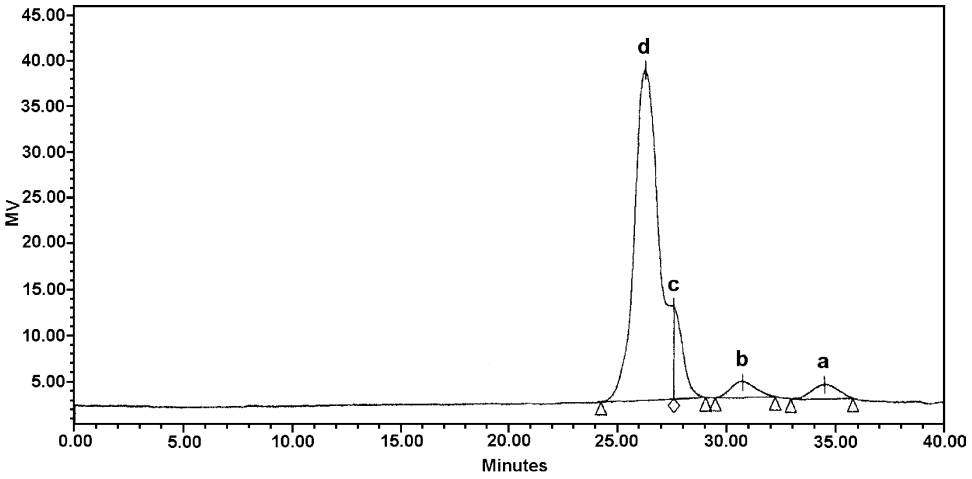

Fig. 2. GPC chromatograms of $(S)_6I(S)_6$.

efficiency of $(S)_4I$ into $(S)_4I(S)_4$ was determined as 73.5% from the GPC chromatogram in Fig. 1(d) based on the magnitudes of the areas underneath the $(S)_4I(S)_4$ and $(S)_4I$ peaks. Besides, a coupling efficiency of $(S)_6I$ into $(S)_6I(S)_6$ as high as 90.8% was attained in our experiments.

Similar variations in the molecular weight distribution of samples taken at the end of each synthesis step were observed for $(S)_6I(S)_6$. A representative GPC-RI chromatogram of $(S)_6I(S)_6$ is given in Fig. 2. While this sample contained residual $(S)_6I$, $(S)_6$, and SSTM which were very difficult to separate out, the area underneath the $(S)_6I(S)_6$ peak amounted to 83% of total peak areas and should, therefore, exhibit characteristic properties of $(S)_6I(S)_6$. Furthermore, the narrow molecular weight distribution of each peak (polydispersity was 1.08, 1.04, 1.01 for peak a, b, c correspondingly) clearly indicated that the samples were essentially nearly monodispersed.

3.2. Characteristics of SSTM and $(S)_nI(S)_n$

Fig. 3 shows the ^{1}H NMR spectrum of the SSTM sample taken after the completion of the *p*-CMS capping on the living polystyrene. The characteristic peaks for the vinyl protons of the terminal styrene unit appear at 5.74 and 5.22 ppm. The methyl proton of the *n*-butyl group from the *n*-BuLi initiator appears at 0.85 ppm. The capping efficiency of the polystyryllithium, or the functionality of the SSTM macromonomer, was then calculated to be 0.94 from the intensity ratio of the vinyl proton and methyl proton peaks [18,25]. Therefore, nearly all polystyrene arms were functionalized and thus were able to form the star polystyrene later.

The ^{1}H NMR spectrum of $(S)_4I(S)_4$ is shown in Fig. 4. The methine proton of the 1,2-polyisoprene appears at 6.1–5.5 ppm and the methine proton of the 1,4-polyisoprene

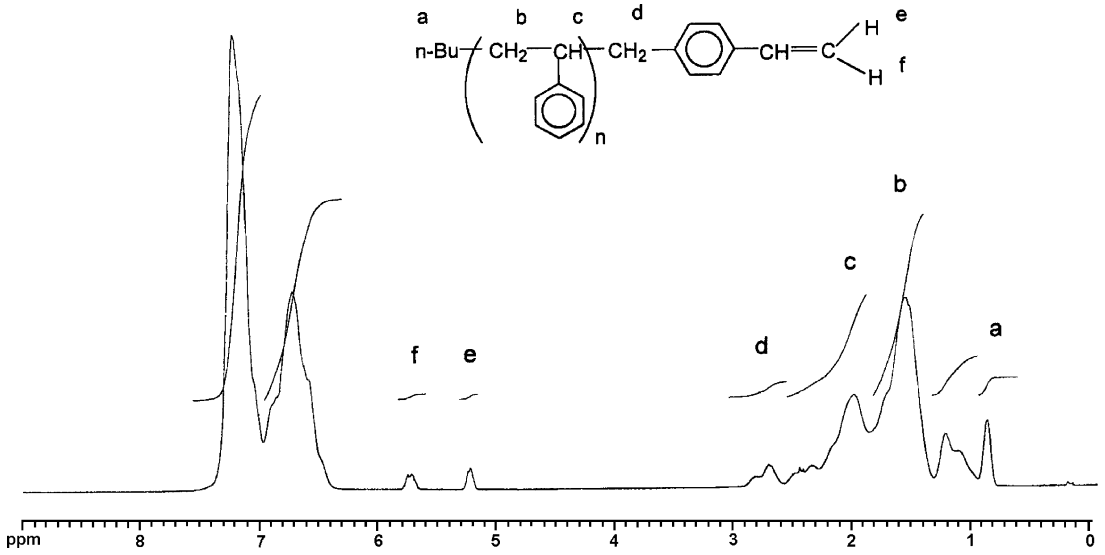

Fig. 3. ^{1}H NMR spectrum of SSTM.

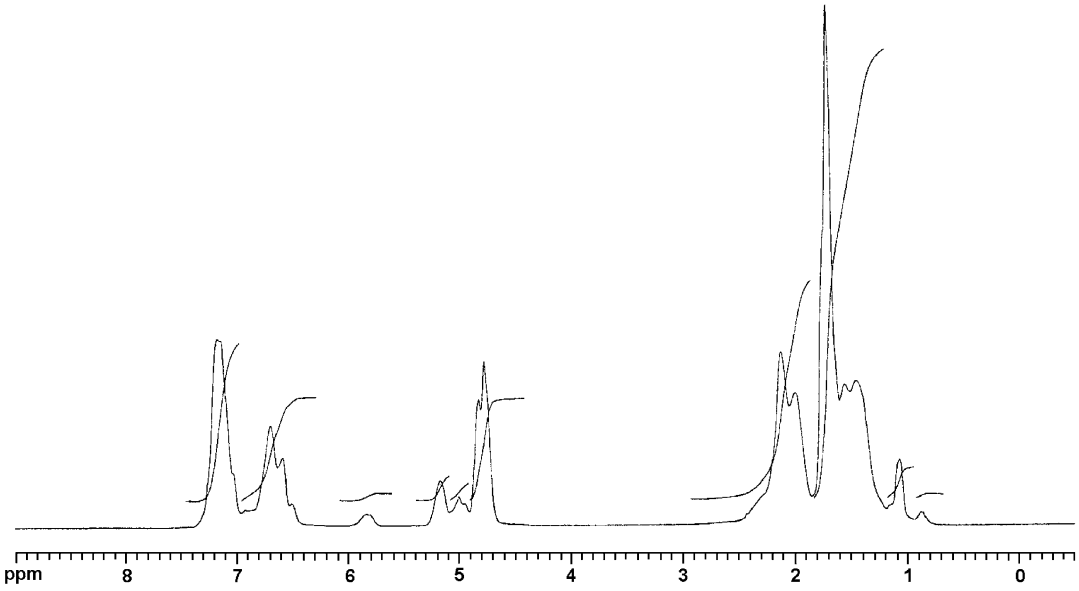

Fig. 4. ^{1}H NMR spectrum of $(S)_4I(S)_4$.

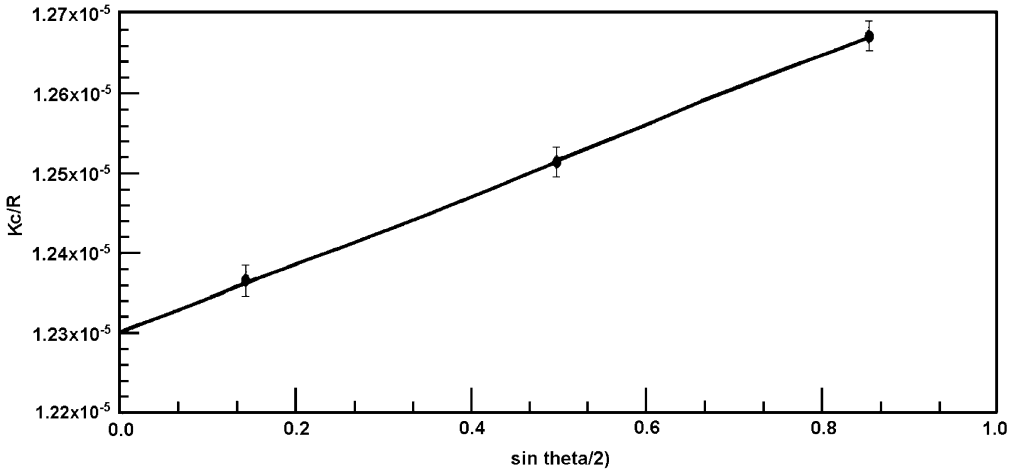

Fig. 5. Debye plot generated by GPC-MALLS for $(S)_6I(S)_6$.

appears at 5.2 ppm. The appearance of these peaks served as an direct evidence for the formation of copolymers.

3.3. Molecular weight of $(S)_nI(S)_n$

The GPC-RI chromatogram was used for the determination of the molecular weights of SSTM, $(S)_n$, $(S)_nI$, $(S)_nI(S)_n$ and the linear SIS analogs (Tables 1 and 2). Since the GPC-RI instruments were calibrated with homopolystyrenes as the standards, the determined molecular weight was actually the 'polystyrene equivalent' molecular weight, or the relative molecular weight. Therefore, the absolute molecular weights of $(S)_nI(S)_n$ and the linear SIS analogs had to be determined with MALLS. Values of the specific RI increment (d*n*/d*c*), which were prerequisite, were measured as 0.1372 and 0.1360 for $(S)_nI(S)_n$ and SIS, respectively.

The Debye plot generated with MALLS for $(S)_6I(S)_6$ is shown in Fig. 5. The good linear fit indicated the accuracy of the MALLS measurements. The characteristic data of $(S)_nI(S)_n$ and the linear SIS analogs measured by GPC-RI

Table 1
GPC-RI results of each SSTM, $(S)_n$, $(S)_nI$ and $(S)_nI(S)_n$

Polymer	$M_n\times10^{-4}$	$M_w\times10^{-4}$
SSTM	0.15	0.16
$(S)_4$	0.54	0.58
$(S)_4I$	1.94	2.01
$(S)_4I(S)_4$	3.91	4.12
SSTM	0.20	0.21
$(S)_6$	1.08	1.12
$(S)_6I$	3.86	3.92
$(S)_6I(S)_6$	8.64	9.70

M_n = relative number average molecular weight, M_w = relative weight average molecular weight, measured by GPC-RI.

Table 2
Characteristics of $(S)_nI(S)_n$ and the linear SIS measured by GPC-RI and GPC-MALLS

Polymer	Content ratio (S:I)	$M_n \times 10^{-4}$	$M_w \times 10^{-4}$	$M_w \times 10^{-4}$	Rg (nm)
$(S)_4I(S)_4$	4:6	3.91	4.12	3.21	5.0
SIS (a)	4:6	4.19	4.38	3.27	5.5
$(S)_6I(S)_6$	3:7	8.64	9.70	8.13	12.6
SIS (b)	3:7	7.27	9.76	8.15	12.9

M_w = absolute weight average molecular weight, measured by GPC-MALLS; the radius of gyration (Rg).

and GPC-MALLS are tabulated in Table 2. The molecular weight (M_w) of the $(S)_nI(S)_n$ and the linear SIS analogs measured by GPC-RI was larger than the corresponding absolute molecular weight (M_w) measured by GPC-MALLS. This was because isoprene had a larger hydrodynamic volume than styrene. In the mean time, the relative molecular weight of $(S)_nI(S)_n$ was smaller than its linear SIS analog, and this was attributed to the smaller radius of gyration (Rg) of star molecules as compared to its linear counterpart.

For block copolymers two composition distributions usually exist over different elution volumes and at the same elution volume, and this has to be considered when the molecular weights are measured. The measured molecular weights should be corrected by a theoretical equation [26]. However, for anionically-synthesized block copolymers in our studies, the composition distribution over the same elution volume is very sharp (because of the living nature of anionic polymerization and the sequential mode of block-forming) and could be ignored,. Furthermore, the narrow molecular weight distribution (with a polydispersity between 1.02 and 1.07 except for $(S)_6$–I–$(S)_6$) made the effect of composition distribution over different elution volumes also negligible.

3.4. Thermal properties

TGA curves of $(S)_nI(S)_n$ and the linear SIS analogs are shown in Fig. 6. The thermal degradable temperature (T_D) of $(S)_4I(S)_4$ and SIS(a) were 358.20 and 349.60 °C; the T_D of $(S)_6I(S)_6$ and SIS(b) were 359.16 and 361.71 °C. Hence, the dependence of thermal stability on the molecular structure was insignificant. Nevertheless, the thermal degradable temperature increased with an increase in the molecular weight of $(S)_nI(S)_n$ or the linear SIS, presumably due to the higher degree of interaction between molecules.

Previous investigations about the stereospecific polymerization of isoprene showed that both the type of initiator and the type of the solvent exerted a profound effect on the microstructure of polyisoprenes [27]. The use of *n*-BuLi as the initiator and cyclohexane as the solvent would lead to the formation of polyisoprene with a microstructure containing 5 mol% 3,4-, 80 mol% *cis*-1,4, and 15 mol% *trans*-1,4 units [27]. Because the same initiator and the solvent were used in our experiments for the synthesis of SIS and $(S)_nI(S)_n$, the *cis*-, *trans*-, and *vinyl* contents of polyisoprene should be alike. Consequently, all properties were compared in the absence of the effect of microstructure difference. The DSC analyses of $(S)_4I(S)_4$, SIS(a), and $(S)_4I$

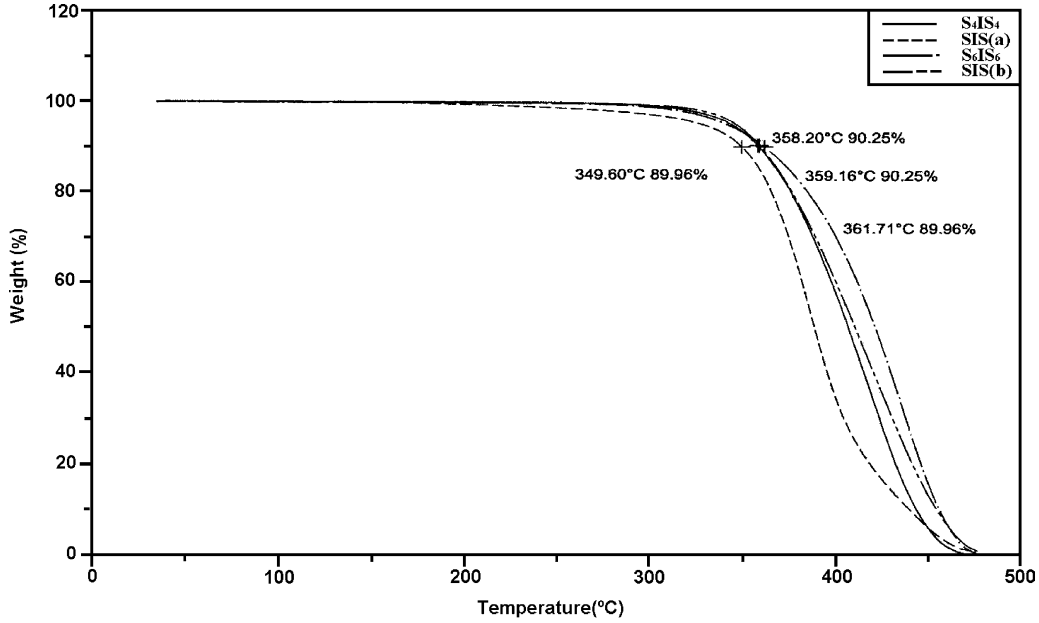

Fig. 6. TGA thermograms of $(S)_nI(S)_n$ and SIS.

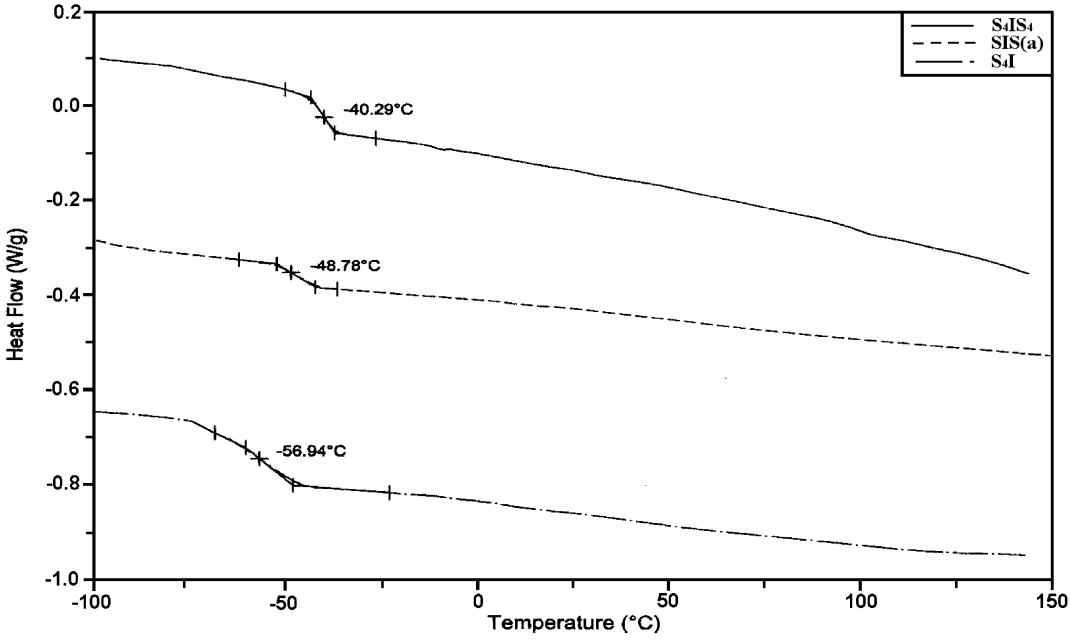

Fig. 7. DSC thermograms of $(S)_4I(S)_4$, SIS(a) and $(S)_4I$.

are shown in Fig. 7. It has long been known that polyisoprene has a lower glass transition temperature (T_g, −73 °C) and polystyrene has a higher T_g (100 °C). In a copolymer such as SIS(a), the T_g of polyisoprene domain would be influenced by the polystyrene domain thus resulting in an increase of T_g (−48 °C), and a low styrene content often made the T_g of polystyrene difficult to detect. Nevertheless, $(S)_4I(S)_4$ had a T_g of −40 °C which was higher than the T_g of its linear SIS(a) analog. This observations could be attributed to the better domain separation in $(S)_4I(S)_4$ due to the expulsive nature of the star-shaped structure. In contrast, the T_g (−56 °C) of the $(S)_4I$ was lower than that of $(S)_4I(S)_4$. This was because the one extremity of $(S)_4I$ was not fixed by polystyrene, therefore, causing a higher internal mobility of polyisoprene chain.

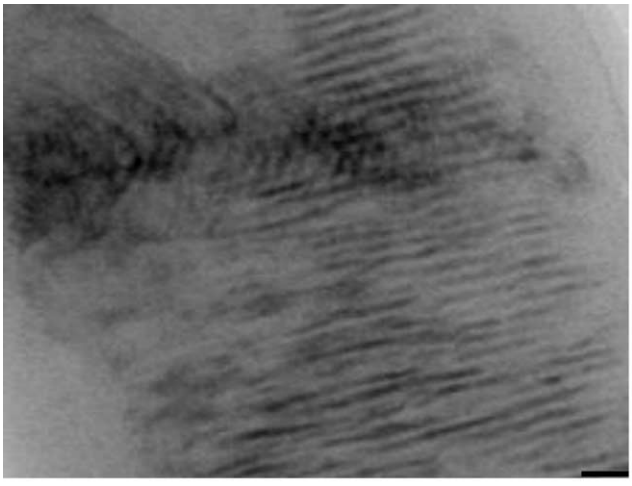

Fig. 8. Transmission electron micrograph of $(S)_6I(S)_6$.

3.5. Morphology

Fig. 8 shows the transmission electron micrograph of the $(S)_6I(S)_6$. Compared to a linear SIS which typically revealed spherical polystyrene microdomains dispersed in the continuous polyisoprene matrix [27], the transmission electron microraph of $(S)_6I(S)_6$ in magnification (×100,000) showed the lamellae-forming phase separation in conjunction with many long-range disorders. Similar morphological changes arising from a change in the composition of block copolymers had been observed previously [28,29]. Polystyrene-*b*-polyisoprene diblock copolymers which contained 31 wt% polystyrene exhibited cylindrical polystyrene microdomains in polyisoprene matrix [28]. At the same molecular weight, polystyrene-*b*-polyisoprene star copolymers comprising 30 wt% polystyrene as outer blocks exhibited a double-diamond microstructure which lies between the hexagonal-packed cylindrical structure and the lamellar structure [29].

3.6. Rheology

The frequency scans were conducted on polymer melts with a rheometer at 100 °C. The logarithm of the loss modulus (G''), the storage modulus (G') and the complex viscosity (η^*) for $(S)_4I(S)_4$ and the SIS(a) are shown in Figs. 9 and 10, respectively. Compared in the low frequency scan range (i.e. in close approximation to the zero-shear viscosity), the $(S)_4I(S)_4$ had a lower viscosity than the linear SIS(a) [30]. This was attributed to the fact that the star shape of the two polystyrene end blocks in each molecule shortened the chain length of the molecule and thus reduced the extent of chain entanglement between molecules.

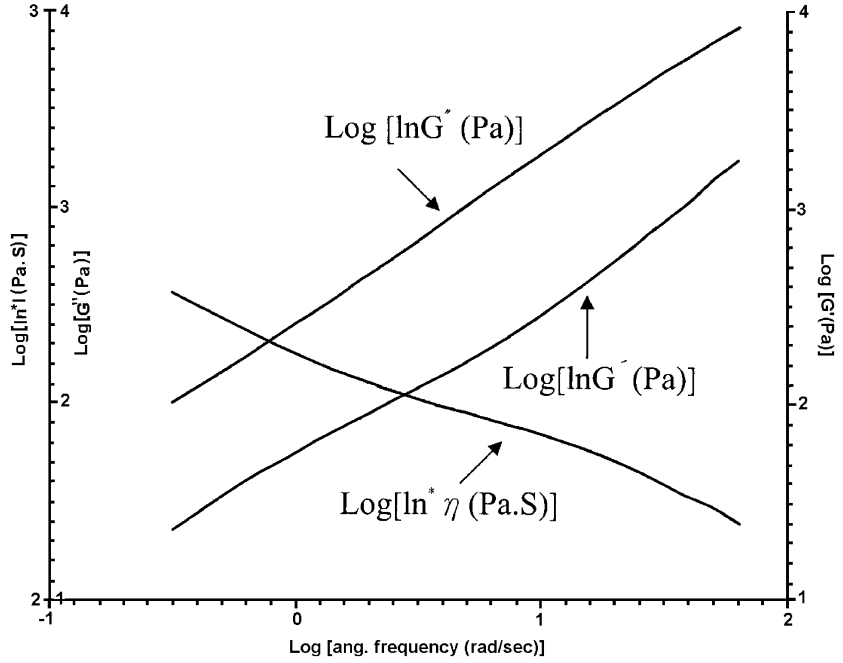

Fig. 9. The frequency scans of $(S)_4I(S)_4$ at 100 °C.

4. Conclusions

The method described in this article enabled us to synthesize a (star polystyrene)-*block*-(linear polyisoprene)-*block*-(star polystyrene) copolymer, $(S)_nI(S)_n$, with a precise control over the number of the arms in the end blocks. While the thermal stability appeared independent of the molecular structure, $(S)_nI(S)_n$ had a higher T_g than the linear SIS with an identical molecular weight. The morphology of $(S)_nI(S)_n$ showed a lamellae-forming phase separation in conjunction with many dislocation defects. The star shape of the two polystyrene end blocks in $(S)_nI(S)_n$ reduced the extent of chain entanglement and, therefore, had a lower melt viscosity than SIS.

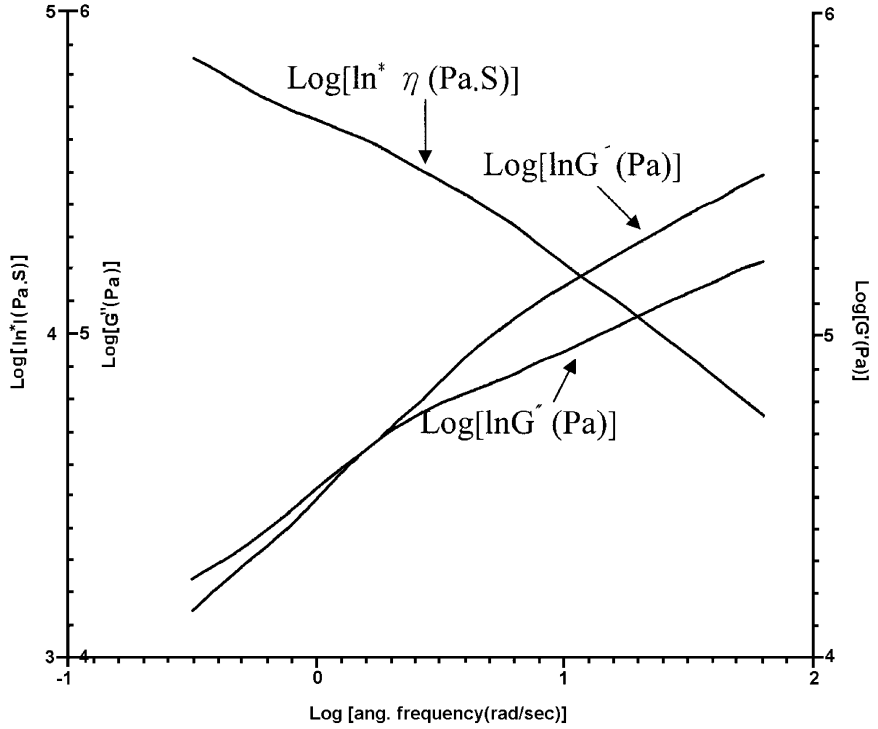

Fig. 10. The frequency scans of SIS(a) at 100 °C.

References

[1] Reiss G, Hurtrez G, Bahadur P. Block copolymers. In: Kroschwitz JI, editor. Encyclopedia of polymer science and engineering. New York: Wiley-Interscience; 1985.
[2] Roovers J, Toporowski PM. Macromolecules 1981;14:1174.
[3] Hakiki A, Young RN, McLeish TCB. Macromolecules 1996;29:3639.
[4] Gido SP, Lee C, Pochan DJ, Pispas S, Mays JW, Hadjichristidis N. Macromolecules 1996;29:7022.
[5] Lee C, Gido SP, Poulos Y, Hadjichristidis N, Tan NB, Trevino SF, et al. J Chem Phys 1997;107:6460.
[6] Iatrou H, Avgeropoulos A, Hadjichristidis N. Macromolecules 1994; 27:6232.
[7] Iatrou H, Willner L, Hadjichristidis N, Halperin A, Richter D. Macromolecules 1996;29:581.
[8] Avgeropoulos A, Hadjichristidis N. J Polym Sci, Part A 1997;35:813.
[9] Roovers J. Macromolecules 1984;17:1196.
[10] Bishko G, McLeish TCB, Harlen OG. Phys Rev Lett 1997;79:2352.
[11] McLeish TCB, Larson RG. J Rheol 1998;42:81.
[12] Bishko GB, Harlen OG, McLeish TCB, Nicholson TM. J Non-Newtonian Fluid Mech 1999;82:255.
[13] Hadjichristidis N, Xenidou M, Iatrou H, Pitsikalis M, Poulos Y, Avgeropoulos A, et al. Macromolecules 2000;33:2424.
[14] Velis G, Hadjichristidis N. Macromolecules 1999;32:534.
[15] Knauss DM, Huang T. Macromolecules 2002;35:2055.
[16] Knauss DM, Huang T. Macromolecules 2003;36:6036.
[17] Tsukara Y, Inoue J, Ohta Y. Polym J 1994;26:1013.
[18] Endo K, Senoo K. Polymer 1999;40:5977.
[19] Al-Muallem HA, Knauss DM. J Polym Sci, Part A 2001;39:152.
[20] Viola GT, Cavallo C. J Polym Sci, Part A 1997;35:17.
[21] Takaki M, Asami R, Ichikawa M. Macromolecules 1997;10:850.
[22] Kaminsky W, Arndt M. Adv Polym Sci 1997;127:143.
[23] Liu IC, Tsiang RCC. J Polym Sci, Part A 2003;41:976.
[24] Kim JK, Lee HH. Macromolecules 1998;31:4045.
[25] Endo K, Senoo K, Takakura Y. Eur Polym J 1999;35:1413.
[26] Se K, Sakakibara T, Ogawa E. Polymer 2002;43:5447.
[27] Morton M. Anionic polymerization: principles and practice 1983, pp. 147–153, 203.
[28] Hasegawa H, Tanaka H, Yamasaki K, Hashimoto T. Macromolecules 1987;20:1651.
[29] Thomas EL, Alward DB, Kinning DJ, Martin DC, Handlin DL, Fetters LJ. Macromolecules 1986;19:2197.
[30] Wang TY, Tsiang CC. J Appl Polym Sci 2001;79:1838.